The (p,α) Reaction

R.K. Bhowmik, R.G. Markham, J.A. Nolen, Jr., M.A.M. Shahabuddin, and P.A. Smith

The (p,α) reaction has a number of useful or potentially useful qualitative features for nuclear structure studies. The fact that this reaction has been previously shown to be a three particle direct pickup reaction, combined with considerations of the associated internal degrees of freedom lead to the following qualitative predictions: 1) Proton hole states are strongly populated. This feature is particularly useful for studying those levels in nuclei that cannot be reached by the (d, ^{3}He) or (t,α) reactions. Coherence in the (p,α) reaction could, in principle, greatly attenuate simple hole states which are strong in single proton pickup reactions: however, no destructive interference of this type has been observed to date. 2) High spin (seniority three) transfer can occur. For example, if three $f_{7/2}$ particles are picked up, transfers of spin up to $19/2^-$ from even-even targets or up to 12^+ from an odd proton $7/2^-$ target are allowed. Part of the incentive for the ^{52}Cr(p,α) study, discussed in more detail below, was to search for the $19/2^-$ state in ^{49}V. 3) $T_>$ states which are the analogues of neutron hole states can be populated with the (p,α) reaction. In our data on targets of ^{52}Cr, ^{44}Ca, and ^{26}Mg such states show up clearly in the spectra.

Another feature of the (p,α) reaction is the well known strong J-dependence observed in the angular distributions for L=1 transitions. It has been known for some time that this effect is due to the spin-orbit potential in the proton channel and that it is not a form factor effect. However, it is not known qualitatively why the effect is so strong in (p,α) as compared to (p,d), for example. We are currently trying to understand this point by looking into the details of DWBA and optical model calculations. There is also calculated J-dependence for higher L-transfers in the (p,α) reaction but it is generally weaker and not well established empirically. Part of the justification of the present study is to accumulate additional data on a wide variety of transitions to states of known spin and parity in order to shed additional light on this problem.

More quantitative interpretation of (p,α) spectra can only come through the development of a microscopic model of the reaction in the context of a nuclear structure model appropriate to the mass region being investigated. A Groningen group has recently had considerable success with a semi-microscopic form factor combined with a weak-coupling nuclear model in the Sn region. We are currently developing a more microscopic model appropriate for use with detailed shell model wave functions. This requires a general microscopic form-factor code for three-nucleon transfer reactions, analogous to what presently exists for two-nucleon transfer. Several prescriptions exist, with the simplest and most widely used being the approximation of mass-3 cluster transfer. This has been fairly successful in fitting shapes of angular distributions, but structure effects arising from interference between various coherent configurations, etc. cannot be included in such a model. The code of Falk at Winnipeg provides form factors in a microscopic description, with arbitrary coupling of the angular momenta of the three picked up nucleons. We have also written a microscopic form factor program, except that we are using the Bayman-Kallio numerical technique rather than the oscillator expansion of Woods-Saxon radial wave functions. The code allows arbitrary neutron couplings and neutron pickup from different shells. It is also possible to use this form factor in a finite range code such as LOLA. At present this new form factor code is running and calculations are presented with some of the specific cases discussed below.

1. ^{52}Cr(p,α)^{49}V

The ^{52}Cr(p,α)^{49}V reaction has been studied at 35 MeV bombarding energy. The reaction products were momentum analyzed in an Enge split-pole spectrograph. A focal plane detector, the delay line counter developed by Markham and Robertson, was used to measure position and energy loss information. The α particles could be easily separated from the intense proton inelastic groups with the energy loss. However, because the proton groups were so intense, and the (p,α) cross sections small, it was necessary to determine the time-of-flight of the reaction products. This was done by starting a TAC with pulses from a plastic scintillator placed behind the counter and stopping the TAC with a signal derived from the cyclotron rf system. The time of flight constraint removed the small number of protons as well as some tritons that overlapped the α-particle energy loss band due to straggling in the ΔE detector.

A typical spectrum is shown in Fig. 1. The strongest states are the $7/2^-$ ground state, the $3/2^+$ level at .748 MeV of excitation, and the 1.646 MeV $1/2^+$ level. These states are dominantly $0f^{7/2}$, $0d^{3/2}$, and $1s^{1/2}$ proton hole configurations.

The back angle spectra are dominated by a different set of peaks (Fig. 2). Low spin states have angular distributions which fall rapidly with increasing angle, while high spin levels have

flatter angular distributions. The large peaks in Fig. 2 are candidates for spin as high as $19/2^-$. Unfortunately, the angular distributions of these states do not resemble the DWBA calculations for the high spin states predicted to be populated via $(f_{7/2})^3$ transfer.

The excitation region from 5.5 MeV to 10 MeV has also been examined. The 55° spectrum is displayed in Fig. 3. The three peaks are apparently the $J^\pi=7/2^-$, $1/2^+$ and $3/2^+$; T=5/2 analogs of neutron hole states in ^{49}Ti.

If the ^{52}Cr(p,α)^{49}V and ^{51}V(p,t)^{49}V spectra are compared, it is seen that a number of peaks in the (p,α) spectra are not observed in the (p,t) spectra. Table 1 contains a list of these levels for all the previously determined levels. In all cases these states have positive parity; i.e., they involved proton configurations which cannot be populated via the neutron transfer reaction.

Table 1: Levels seen in ^{52}Cr(p,α)^{49}V that are not in ^{51}V(p,t)^{49}V.

Excitation Energy	J^π
0.748	$3/2^+$
1.141	$5/2^+$
1.602	$7/2^+$
1.646	$1/2^+$
1.995	$3/2^+$
2.388	$5/2^+$

If the comparison is reversed, we find that there are levels observed in the (p,t) experiment that are not in the (p,α) spectra. Indeed, some of these levels are also seen in ^{50}Cr(t,α)^{49}V spectra. It must be concluded that coherence in the (p,α) reaction can attenuate greatly the yields to certain states.

Zero-range DWBA calculations have been performed with two form factor models. The lowest ten levels are fit with mass three cluster form factors in Fig. 4. The fits are reasonably good. We have found that the fits to the $7/2^-$ and $11/2^-$ angular distributions can be improved by using a smaller diffuseness. This is done, however, at the expense of the $1/2^+$ and $3/2^+$ fits.

The cluster model cannot be easily related to shell model wave functions. In order to relate the strengths of the simple transitions to pure shell model configurations, it is necessary to use a microscopic form factor. We have derived such form factors from a generalization of the Bayman-Kallio two nucleon transfer technique. The fits to the lowest ten levels, shown in Fig. 5, are not qualitatively better or worse than those for mass 3 cluster transfer.

If the three hole states are assumed to be simple proton holes, the zero-order theory predicts the relative spectroscopic factors of the $7/2^-$, $3/2^+$, and $1/2^+$ transitions to be 1.0, 1.0 and 0.5 respectively. Table 2 gives a list of the expected values and the experimental values. The agreement is good considering the simple structures assumed for these states.

Table 2: Relative Spectroscopic Factors for the Proton Hole States

Excitation Energy	J^π	Theory	Measured
0.000	$7/2^-$	1.0	1.0*
0.748	$3/2^+$	1.0	.84
1.646	$1/2^+$	.5	.54

*Normalized to one. All other values relative to this.

2. ^{44}Ca(p,α)^{41}K

Previous (p,α) studies have concentrated on configurations where the two neutrons that are picked-up come from the same shell. The low lying $7/2^-$ level that is found in the potassium isotopes presents a chance to study a transition that may involve different neutron shells. Population of this level may be the result of picking up neutrons from the $f_{7/2}$ and $d_{3/2}$ orbitals, and a $d_{3/2}$ proton, or it may be populated via a proton two particle-two hole proton admixture in the ^{44}Ca ground state.

We have studied the ^{44}Ca(p,α)^{41}K reaction at E_p=35 MeV for the purpose of concentrating on the negative parity final states. In addition we have determined a number of spins and parities of the ^{41}K levels.

A typical spectrum is shown in Fig. 6. The largest peak in the spectrum had not been previously reported. The excitation energy for this peak is about 3.52 MeV. On the basis of its strength and angular distribution it appears to be a $5/2^+$ proton hole state.

The 1.293 MeV, 7/2- state is the only negative parity state that is observed definitively. Levels at 3.86 MeV and 4.44 MeV are also seen. These states were previously reported in ^{40}Ar(^{3}He,d)^{41}K where they were assigned ℓ = 3 and 1 respectively. The angular distribution which we obtain for these two levels do not look like any of the ℓ = 3 or 1 DWBA calculations which we have performed. The best fits seem to be with $5/2^+$ and $3/2^+$ calculation.

The proton hole strength does not appear to be concentrated in single peaks in the ^{41}K spectrum. Although the strongest peaks in Fig. 6 are the $3/2^+$ ground state, the $1/2^+$ level at 0.980 MeV, and the 3.52 MeV, $5/2^+$

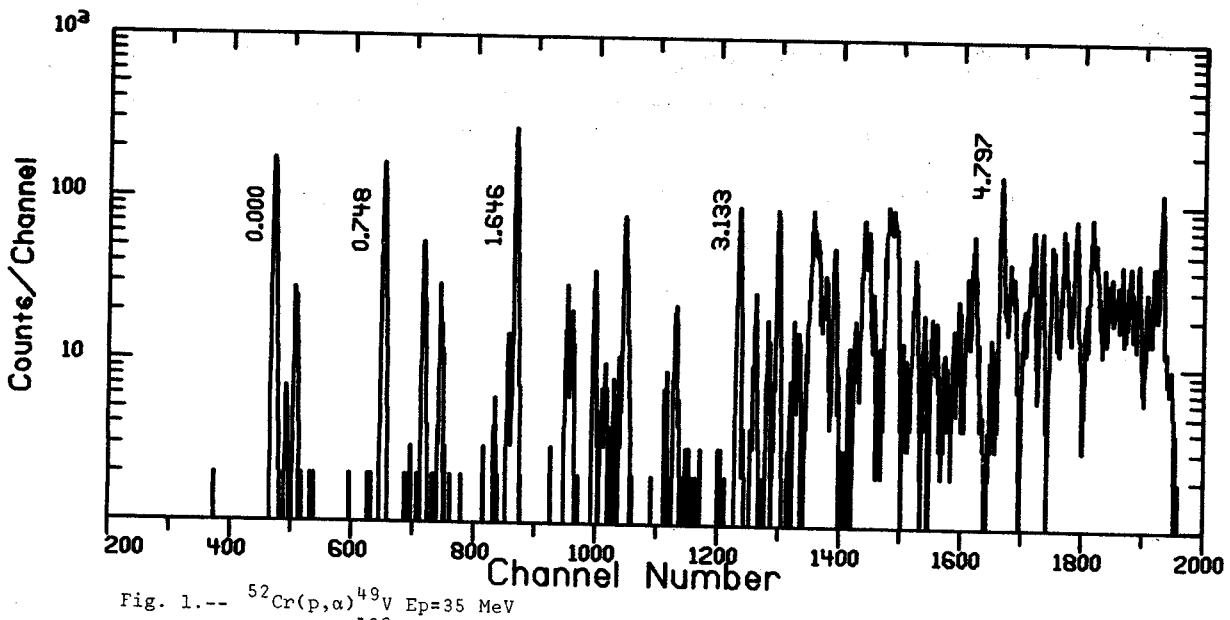

Fig. 1.-- $^{52}Cr(p,\alpha)^{49}V$ Ep=35 MeV 16°

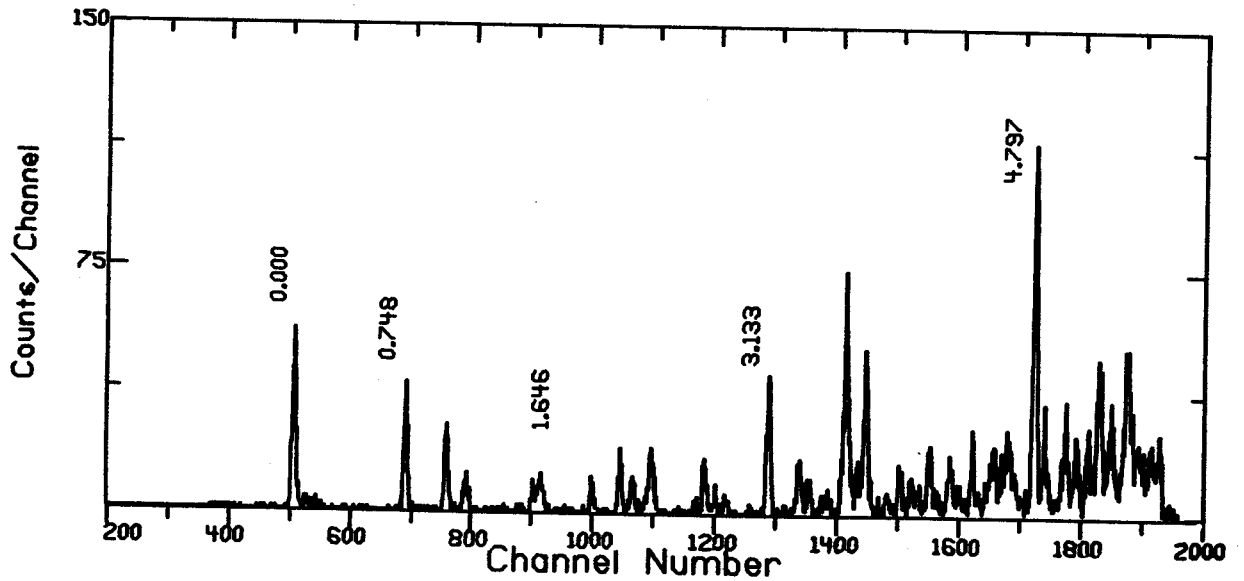

Fig. 2.-- $^{52}Cr(p,\alpha)^{49}V$ Ep=35 MeV 60°

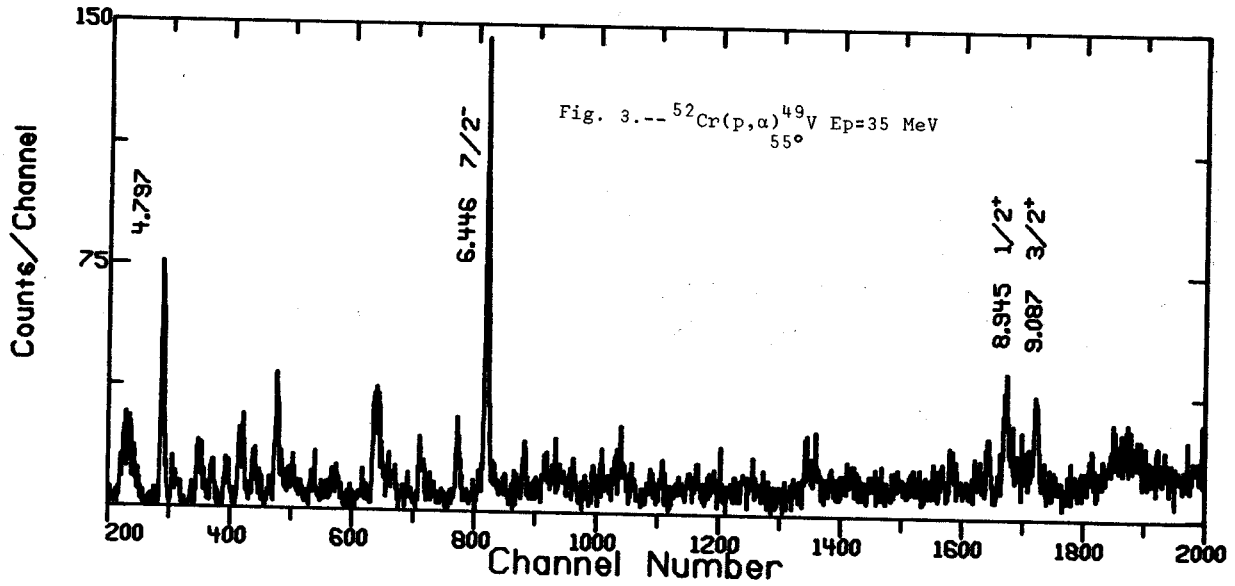

Fig. 3.-- $^{52}Cr(p,\alpha)^{49}V$ Ep=35 MeV 55°

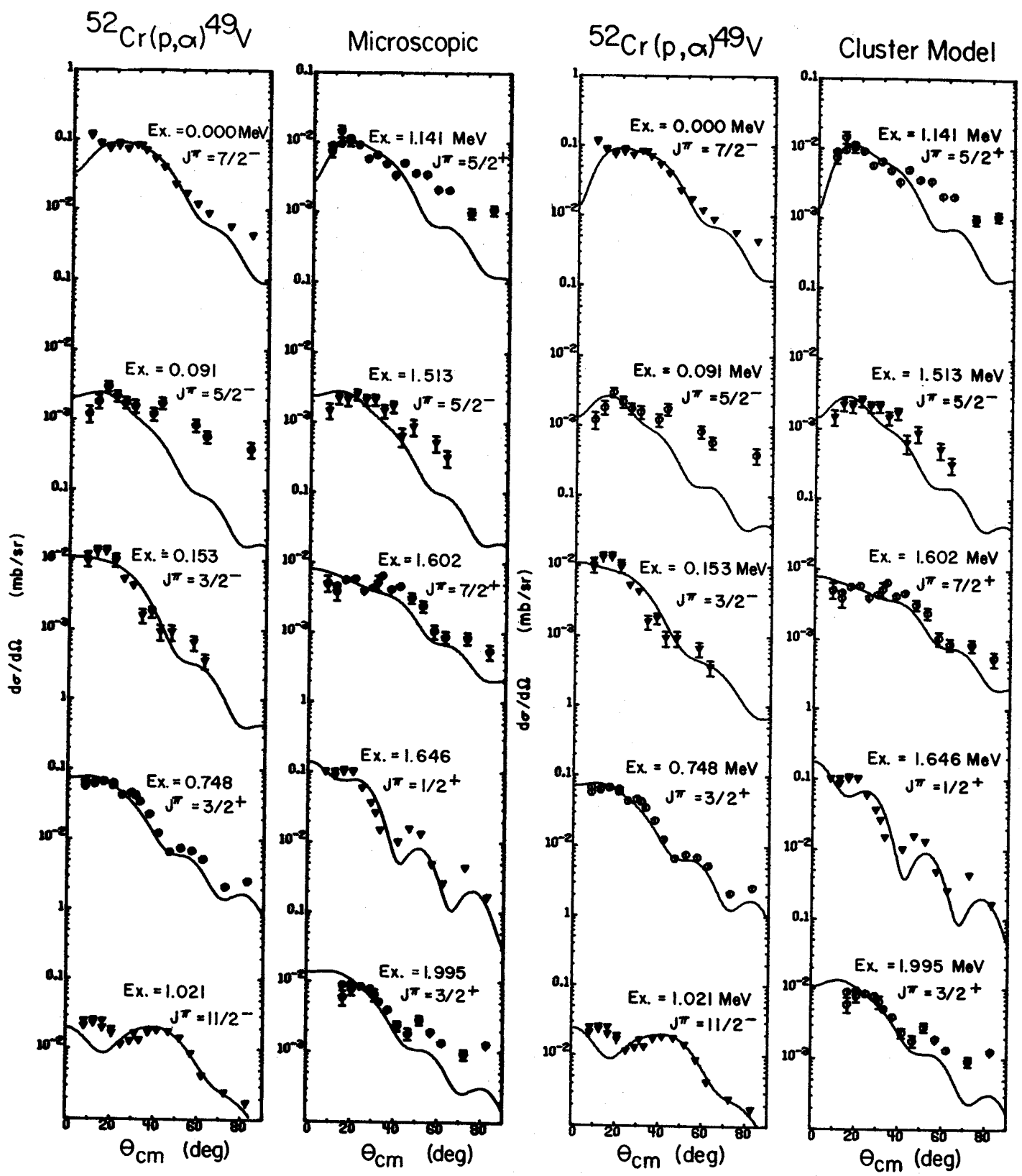

Fig. 4 & 5.--DWBA Calculations

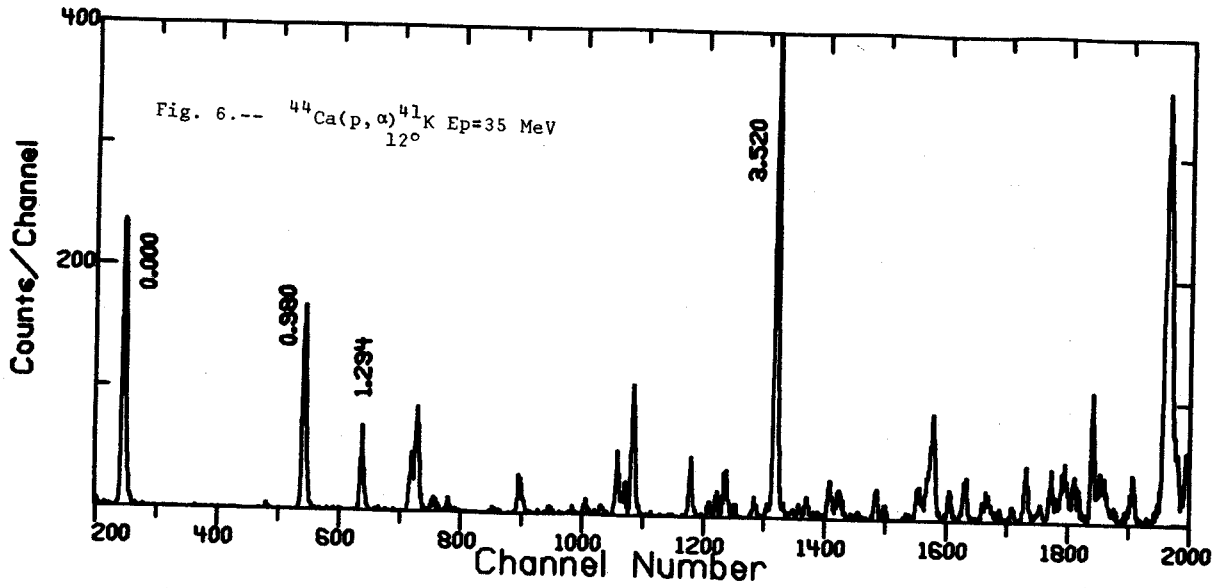

Fig. 6.-- $^{44}Ca(p,\alpha)^{41}K$ Ep=35 MeV 12°

Fig. 7.-- $^{44}Ca(p,\alpha)^{41}K$ Angular Distributions

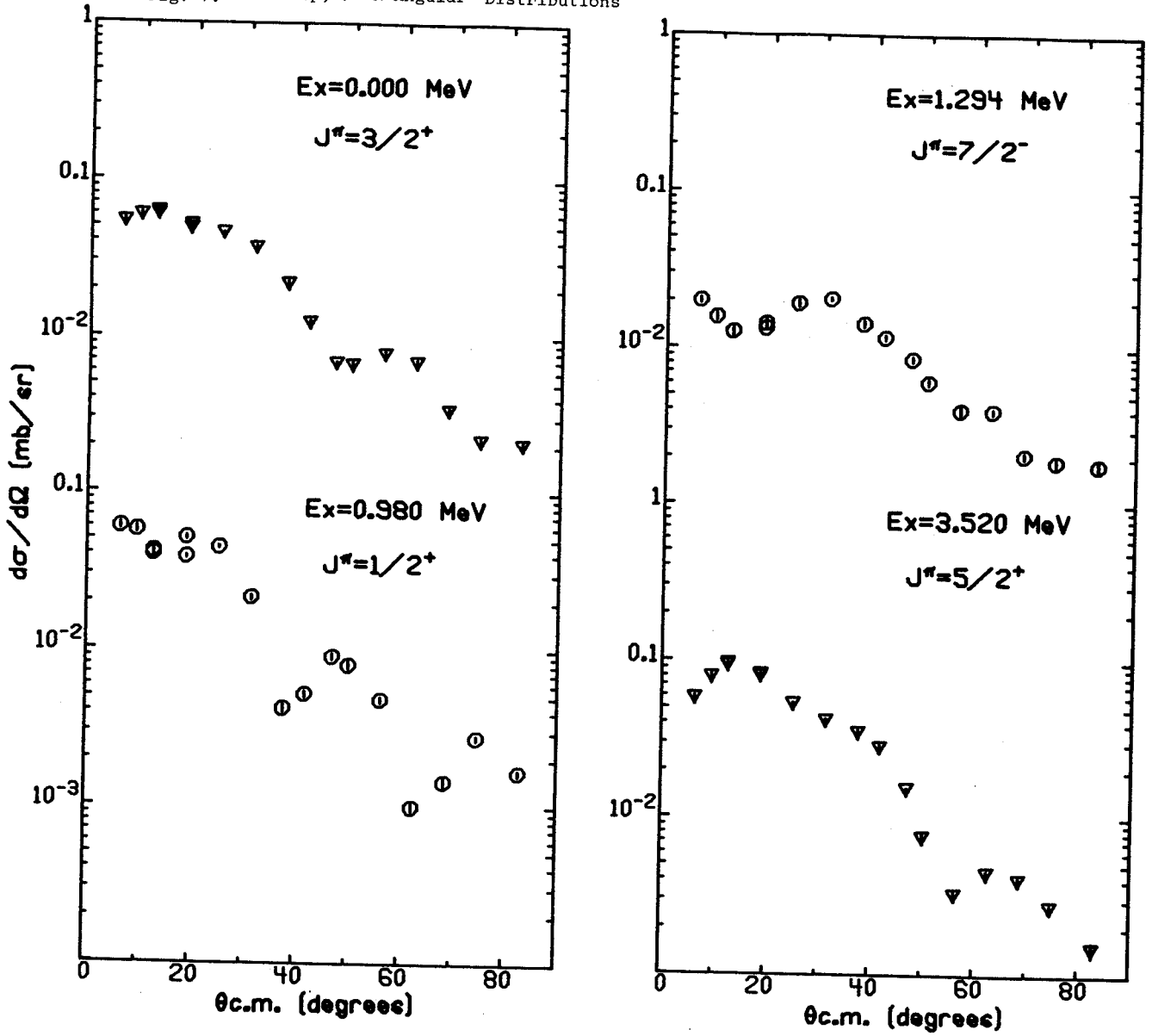

level, these are not all of the strong states. For example, there are three other $1/2^+$ states observed. Two of these, located at 1.59 MeV and 2.67 MeV are nearly half as strong as the peak at 0.98 MeV. The peak at 2.75 MeV is probably a $5/2^+$ level. It is about one third as large as the large peak at 3.52 MeV.

Some of the angular distributions are shown in Fig. 7. DWBA analysis is currently in progress.

3. Proton hole states of ^{119,121}Sb seen via the (p,α) Reaction

Antimony has only one proton in the open orbits past the closure at Z = 50; hence its spectrum should be simply one of proton single-particle states coupled to neutron excitations. However, the spectrum is known to be far more complex. In particular, proton two-particle, one-hole excitations are known to be low lying in ^{121}Sb and the heavier antimony isotopes. These states have been identified by proton pickup from the appropriate tellurium targets and so are not known for the lighter isotopes where suitable targets don't exist. The (p,α) reaction favors the population of proton hole states because the most favored configuration of the transfered particles is one with the neutrons paired to zero angular momentum. Thus, via the (p,α) reaction, we can extend our knowledge of the hole states to include ^{119}Sb. Other

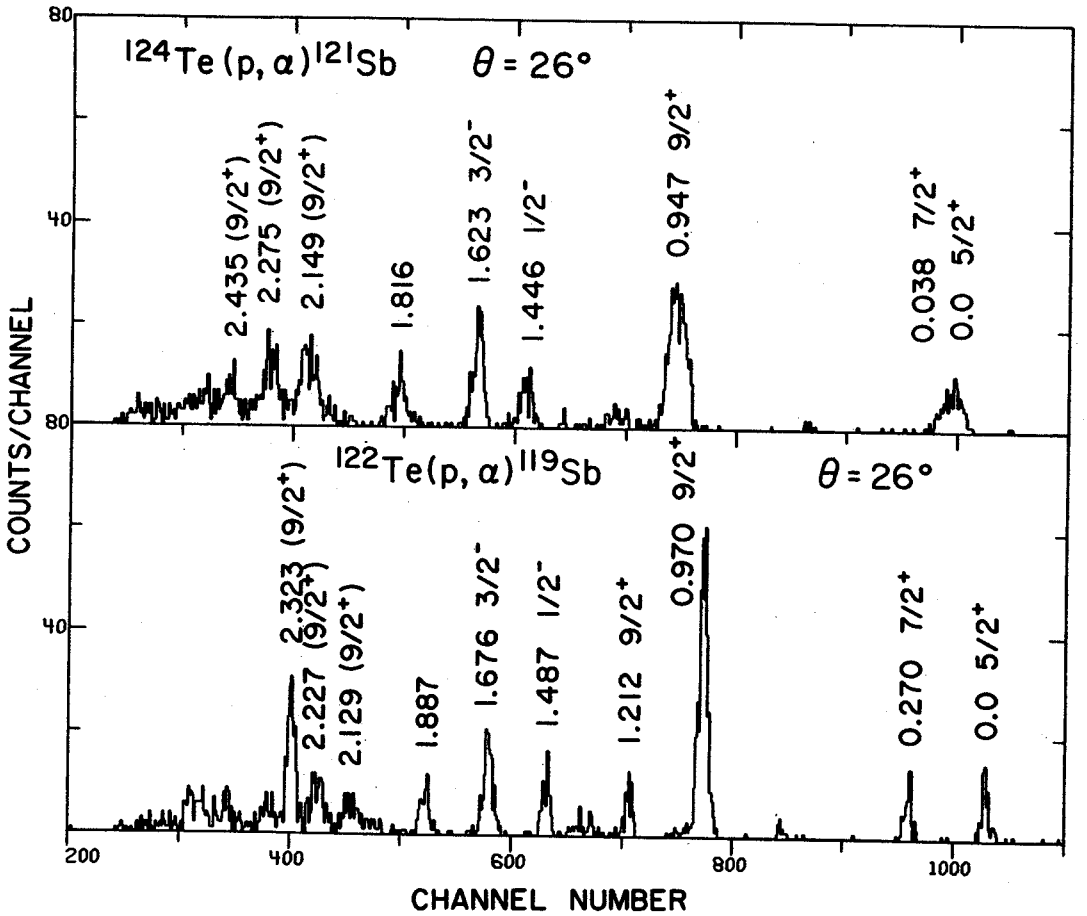

Fig. 8. ^{122,124}Te(p,α) spectra taken at 26° in the lab. The poorer resolution obtained in the ^{124}Te experiment is due to target thickness.

states also will be populated, albeit, with reduced cross sections.

The experimental procedure was the same as for the other (p,α) reactions studied except for difficulties with the targets. Because of the high vapor pressure of tellurium, the target thickness decreased steadily during each run. Thus, it was necessary to rely exclusively on the 90° monitor detector for normalization and to reposition (or change) the target periodically. Absolute cross sections were not obtained with any certainty, but the relative normalization between angles was very reproducible.

Detailed angular distributions were taken on both ^{122}Te and ^{124}Te. In this way, analogous states in both ^{119}Sb and ^{121}Sb could be identified and the character of the ^{119}Sb states established independently of the DWBA calculations.

Spectra taken at 26° lab. angle are shown in Fig. 8. The lowest $J^\pi = 9/2^+$ hole states are most prominent and the $J^\pi = 1/2^-$ and $3/2^-$ peaks are still large even though they peak sharply at more forward angles. The state at 0.970 MeV in ^{119}Sb was known to have $J^\pi = 9/2^+$. This work confirms its $g_{9/2}^{-1}$ character. The identification of the states at 1.487 and 1.676 MeV as the $p_{1/2}^{-1}$ and $p_{3/2}^{-1}$ proton hole states is based on this work. The angular distributions for these states are shown in Fig. 9 along with those of the corresponding states in ^{121}Sb. These angular distributions are characteristic of the J transfer. Furthermore, the corresponding hole states in both nuclei have angular distributions with essentially the same magnitudes and with identical shapes.

A plot of the excitation energies of the hole states (relative to the first $J^\pi = 5/2^+$ state) versus mass for the antimony isotopes is shown in Fig. 10. By including the ^{119}Sb hole states and candidates for lighter isotopes, interesting systematics emerge. The hole states rise in excitation energy when the neutron number approaches sixty-four and eighty-two and lie low in between. The rise at N=82 is most marked since this is a major shell closure. At N=64 the $d_{5/2}$ orbit fills. Apparently this minor closure is complete enough to cause a 500 keV shift of the proton hole states.

The angular distributions have been successfully fitted with cluster-transfer DWBA calculations; further analysis is underway.

4. (p,α) on s-d Shell Nuclei

For nuclei in the s-d shell region, large basis shell model wavefunctions are now available. It therefore seems reasonable to test the reaction mechanisms for the (p,α) reaction in this mass region. We have measured (p,α) angular distributions at 35 MeV for the even-even targets ^{24}Mg, ^{26}Mg and ^{30}Si.

For the reaction ^{26}Mg (p,α)^{23}Na, the final nucleus is particle stable up to 8.79 MeV. To take data over the whole range of excitation energy, two different magnetic field settings were used for the spectrograph, spanning the excitation energy range 0-5 and 5-10 MeV. In a separate run, photographic plates were used to detect the α-particles to measure the energy levels with an accuracy better than 5 keV.

A typical spectrum for ^{24}Mg(p,α)^{21}Na is shown in Fig. 11. ^{21}Na becomes particle unstable at 2.43 MeV excitation energy. Strong unbound states are seen at excitation energies of 5.814, 6,553, 6.656 and 6.939 MeV.

The spectrum from the reaction ^{26}Mg(p,α)^{23}Na is shown in Fig. 12. The peak at 7.888 MeV is the lowest T=3/2 state in ^{23}Na and is the isobaric analog of the g.s. of ^{23}Ne. The 2.704 MeV ($9/2^+$) and 6.236 MeV ($13/2^+$) states are strongly excited in the (p,α) reaction. The yields to states that require seniority three transfer are comparable to those in which seniority one is allowed.

The angular distributions of the low lying states of ^{21}Na, ^{23}Na and ^{27}Al are shown in Fig. 13. The angular distributions of the states of the same spin parity in different nuclei are quite similar, indicating similar configurations of the states.

For reactions involving single nucleon transfer, the angular distribution depends mainly on the L transfer of the reaction. In the case of (p,α) reaction on s-d shell nuclei, states of the same spin parity that are excited quite strongly do not necessarily have similar angular distributions, as can be seen in Fig. 14.

We are at present doing DWBA calculations using microscopic form factors to predict the variations in the shapes of angular distributions. The predicted shapes are extremely sensitive to the α-optical potential used. A qualitative agreement in the relative cross sections of the states in ^{21}Na and in ^{23}Na has been observed.

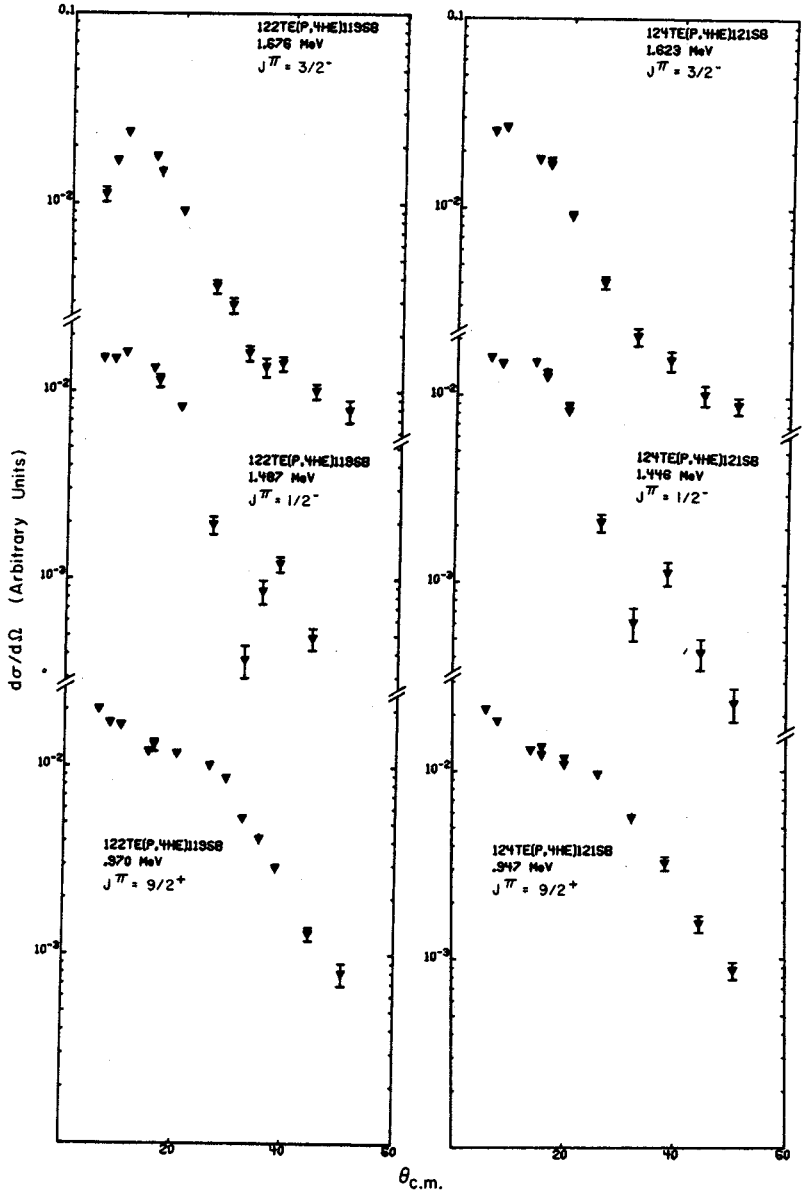

Fig. 9.--Angular distributions for the proton hole states. The similarity of the corresponding angular distributions makes possible the new $J^{\pi}=1/2^{-}$ and $3/2^{-}$ assignments in ^{119}Sb.

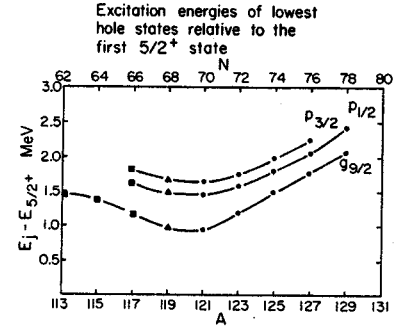

Fig. 10.--The excitation energies of the hole states relative to the first $J^{\pi}=5/2^{+}$ state are plotted versus mass number. The dots represent previous assignments, the triangles are assignments of J^{π} or character (hole state) based on this work and the squares are possible candidates based on gamma ray work (see elsewhere in this report).

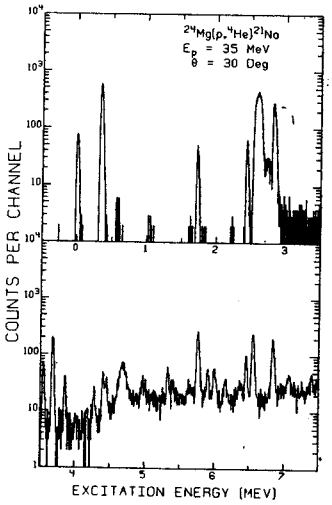

Fig. 11.--^{24}Mg(p,α)^{21}Na spectrum at 30 deg.

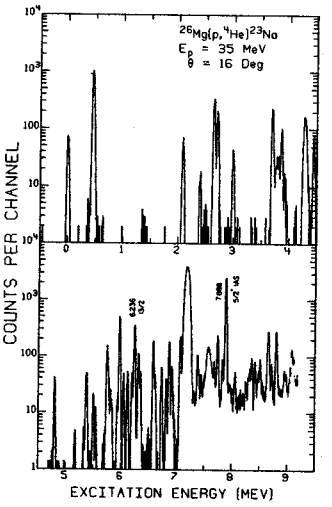

Fig. 12.--^{26}Mg(p,α)^{23}Na spectrum at 16 deg.

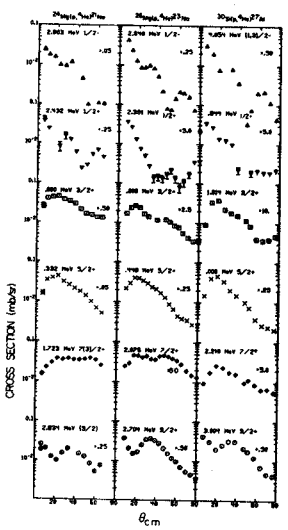

Fig. 13.--Angular distributions for strong sd-shell states.

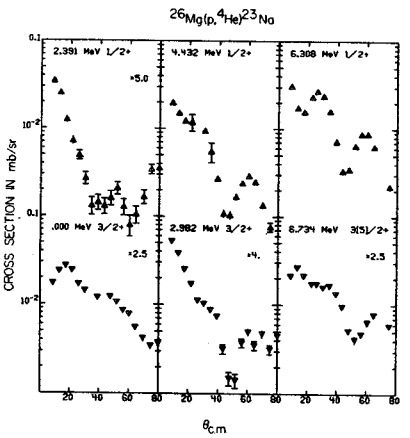

Fig. 14.--Comparison of angular distributions for states with some j^{π}.

Measurement of $V_{\sigma\tau}$ with the ^{7}Li(p,n)^{7}Be (0.000, 0.43 MeV) Reactions at E_p=25, 35, and 45 MeV

R.R. Doering, L.E. Young, R.K. Bhowmik, S.M. Austin, S.D. Schery, and R. DeVito

The central-force charge-exchange part of the effective nucleon-nucleon interaction may be written in the phenomenological form

$$t_{ij} = (V_\tau + V_{\sigma\tau}\vec{\sigma}_i\cdot\vec{\sigma}_j)\vec{\tau}_i\cdot\vec{\tau}_j g(r_{ij}).$$

With the previous MSU neutron time-of-flight (TOF) facility, the magnitude of V_τ was determined through (p,n) cross-section measurements for $0^+\rightarrow 0^+$ isobaric-analog-state transitions at E_p=25, 35, and 45 MeV[1]. The new "beam-swinger" TOF system, which is described in the instrumentation section of this report, is capable of resolving many transitions which are sensitive to $V_{\sigma\tau}$.

A particularly favorable case for the study of $V_{\sigma\tau}$ is ^{7}Li(p,n)^{7}Be (0.00, 0.43 MeV). Anderson, Wong, and Madsen have shown that the ratio of the (p,n) cross sections to the ground and first excited states of ^{7}Be is given in the monopole approximation by[2]

$$\frac{\sigma_0}{\sigma_1} = \frac{V_\tau^2 + 1.47\ V_{\sigma\tau}^2}{1.27\ V_{\sigma\tau}^2}\ .$$

This expression is essentially model independent, since the same distorted waves and form factors have been assumed to describe the (p,n) transitions to both final states and the spectroscopic amplitudes have been derived from the corresponding β-decay rates. Since the cross-section ratio gives the ratio of $V_{\sigma\tau}$ to V_τ, the ^{7}Li(p,n)^{7}Be (0.00, 0.43 MeV) data which we have recently acquired at E_p=25, 35, and 45 MeV nicely complements our previous measurements[1] of V_τ to determine the magnitude of the spin-flip, in addition to the non-spin-flip, component of the central charge-exchange force over this energy range.

The analysis by Anderson, Wong, and Madsen of their data from E_p=9.8 to 19.6 MeV yields $V_{\sigma\tau}/V_\tau$=0.66±0.08. Unfortunately, they were unable to resolve the ground state of ^{7}Be from the 0.43-MeV state at proton bombarding energies above 14 MeV and had to rely on a less certain relationship involving ^{6}Li(p,n)^{6}Be cross sections and the rate of ^{6}He→^{6}Li beta decay. As the ^{7}Li(p,n)^{7}Be spectrum in the instrumentation section of this report demonstrates, we were able to cleanly resolve the ground and 0.43-MeV states all the way up to E_p=45 MeV (E_n≈43 MeV). Our angular distributions at E_p=25 MeV are shown in Fig. 1. The similarity in shape certainly supports the approximation of identical distorted waves and form factors for these two reactions. At the higher bombarding energies, the angular distributions have less structure and fall more rapidly beyond the forward-angle peak.

A preliminary analysis of our data yields $V_{\sigma\tau}/V_\tau$=0.69, 0.78, and 0.87 at E_p=25, 35, and 45 MeV, respectively. The corresponding values of $V_{\sigma\tau}$ (using our previous measurements[1] of V_τ) are 11.7, 11.9, and 12.7 MeV for g(r)=exp(-r)/r, which compare favorably with 12±2.5 MeV, an average of results from other sources.[3] A more detailed analysis based on realistic DWBA calculations including non-central forces is currently in progress.

References

1. R.R. Doering, D.M. Patterson, and Aaron Galonsky, Phys. Rev. C12,378(1975).

2. J.D. Anderson, C. Wong, and V.A. Madsen, Phys. Rev. Lett. 24,1074(1970).

3. S.M. Austin, in The Two-Body Force in Nuclei, edited by S.M. Austin and G.M. Crawley (Plenum, New York, 1972).

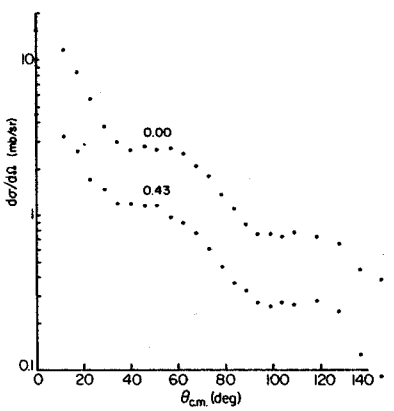

Fig. 1.--Angular distributions for ^{7}Li(p,n)^{7}Be (0.00, 0.43 MeV) at E_p=25 MeV.

Experimental and Theoretical Cross Sections for $^{144}Sm(\tau,xn+\alpha yn)$ Reactions

R.B. Firestone, Wm.C. McHarris, and W.H. Kelly

The study of nuclei far from stability has been an area of extreme interest at the MSU Cyclotron Laboratory. Our pioneering work in the development of rabbit, gas transport, and mass time of flight systems has provided us with powerful tools for the investigation of short-lived activity. A particularly useful beam for these studies is the 76 MeV τ beam which can evaporate up to 8 neutrons or charged particles from a rare earth compound nucleus. The greatest problem in these studies is that it is usually impossible to produce the isotope of interest cleanly. The various activities produced may be sorted out by half-life, x-ray or γ-ray coincidence, chemistry, mass analysis, and excitation function experiments. In order to make use of excitation function data, it is necessary to have a good theoretical understanding of the various reaction cross sections. This theoretical knowledge is also important for choosing the appropriate beam energy in order to optimize production of the activity of interest.

An important tool for calculating the theoretical cross sections is the computer code ALICE by Blann and Plasil.[1] This code calculates compound nuclear reaction cross sections including neutron, proton, and alpha particle channels as well as fission competition. Our experience has shown that ALICE works quite well for simple, low energy reactions, but we are concerned about its value for the more exotic reactions. In order to test the ALICE predictions, excitation functions for 30-70 MeV_τ on $^{144}Sm_2O_3$ were performed and the productions of $^{142,143}Gd$ and $^{140,141}Sm$ were monitored. Activity produced was transported by our He Jet system[2] to a Ge(Li) γ-ray detector where γ-rays from the activities of interest could be followed as a function of beam energy. The spectra were normalized with respect to ^{14}O production, a reaction whose cross section should not change rapidly with respect to beam energy.

The experimental and theoretical cross sections are shown in Fig. 1. As absolute cross sections were not measured, the data was normalized to theory, and all cross sections shown in Fig. 1 are arbitrarily normalized. The (τ,xn) reactions agree quite satisfactorily with ALICE, and the $(\tau,\alpha yn)$ agree equally well including substantiation of the double peak in the excitation function. This double peak results because both an alpha particle and 2p2n can be evaporated by the compound nucleus, however, the two reaction peaks will differ in energy by approximately the binding energy of the alpha particle. These results have increased our confidence in ALICE as a useful experimental tool. We believe that ALICE will be useful both for our work, and for future heavy ion studies which may open up even more exotic nuclei to study.

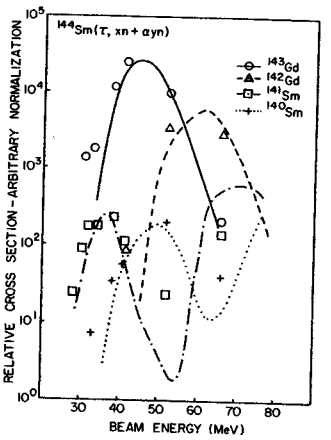

Fig. 1 Theoretical and experimental cross sections for $^{144}Sm(\tau, xn+\alpha yn)$ reactions.

1. M. Blann and F. Plasil, nuclear evaporation code ALICE, adapted for the MSU Cyclotron Laboratory Sigma-7 computer by W. Bentley

2. K.L. Kosanke, Ph.D. Thesis, Michigan State University, 1973.